Contention Resolution in Optical Burst Switched Networks using Spectral-Amplitude-Coding Optical Code Division Multiple Access

Mohamed Y. S. Sowailem, *student member*, IEEE, Mohamed H. S. Morsy, *student member*, IEEE, and Hossam M. H. Shalaby, *Senior member, IEEE*

ABSTRACT

We propose the implementation of spectral-amplitude-coding optical code division multiple access (SAC-OCDMA) as a contention resolution technique in optical burst switched (OBS) networks. The new system architecture is presented in details where an all-optical methodology for cancelling multiple access interference is proposed. Performance evaluation of the proposed system in both MAC and optical layers is introduced where the overall burst error rate of the system is evaluated in three cases: full, partial, and no code conversion capabilities taking into account the receiver dark current, thermal, and shot noises at the egress nodes. Our results reveal that a considerable improvement in the performance of each core node in the system is achieved by using SAC-OCDMA instead of WDM in the optical layer underneath an OBS based MAC layer. We also conclude that a slight increase in the employed number of code converters enhances the overall system performance noticeably. Finally, optimum values for the number of codes, which lead to minimum overall burst error rate, are reached at different traffic conditions.

I. INTRODUCTION

The tremendous increase of the data rate demand necessitates utilizing the vast bandwidth available on optical fiber links which makes it obligatory to realize the dream of all optical networks (AONs). One of the approaches that target this goal is a paradigm called optical burst switching (OBS) which was first proposed in literature by Qiao and Yoo [1]. In OBS, switching is made on a burst by burst basis where the burst comprises of a group of aggregated packets having the same destination and class.

One-way reservation protocols such as Just-In-Time (JIT) and Just-Enough-Time (JET) are commonly used for signaling in OBS. In these protocols, for each burst transmission, one control packet (CP) is sent on a separate control channel prior to the burst with an offset time equals to the processing time of its corresponding CP in the intermediate stages in order to reserve resources for the ensuing data burst (DB). In our paper, we propose some modifications to the information carried by the CP in order to be appropriate with the newly added OCDMA scheme.

The OBS network architecture, as explained in [2], mainly consists of three components; ingress nodes, core nodes and egress nodes. The ingress node is the gate through which the DB enters the network after the aggregation of the data packets. The core node is the node at which the CP is processed reserving appropriate resources for the upcoming DB and configuring the switch fabric to bypass the DB upon its arrival to the destined port. The egress node is the destination node at which the DB is disassembled into original packets, each of which is directed to its own destination.

Although JET and JIT protocols are characterized by small latency, the major hurdle that hinders these protocols is the unacceptable loss probability due to contention between two CPs which may occur while reserving similar resources for their upcoming DBs at the same time. Various techniques were proposed for contention resolution to reduce the burst dropping probability. These techniques are based on multiplexing the contending DBs in either the wavelength domain using wavelength converters, the time domain using fiber delay lines (FDLs) or the spatial domain using the deflection routing scheme.

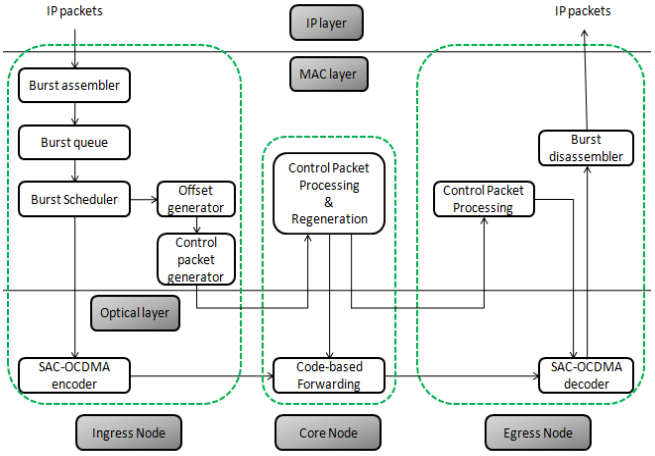

Fig.1. Layers of the OBS/SAC-OCDMA system.

In [3], Kamakura *et al.* proposed using OCDMA as a contention resolution scheme where the multiplexing is done in the code domain. Specifically, Kamakura *et al.* presented a new QoS differentiation scheme by embedding codewords with priority-dependent weights in a single used optical orthogonal code (OOC). However, the paper did not give a detailed description for the architecture of the proposed system. Furthermore, the DB in their system experiences multiple access interference (MAI) from other users on the same OOC which negatively affects the throughput.

The aim of this paper is to propose the implementation of spectral-amplitude-coding optical code division multiple access (SAC-OCDMA) as a new contention resolution technique in OBS. The main idea in the newly proposed system (OBS/SAC-OCDMA) is to increase the number of available resources (codes) for reservation instead of the more limited resources (wavelengths) while using OBS/WDM. The SAC-OCDMA scheme is characterized by the zero MAI feature when using the balanced receiver structure [4]. Inspired by the zero MAI feature and the possibility to increase the code length, hence accommodating more simultaneous users, we propose the new system (OBS/SAC-OCDMA) in order to reduce the overall burst error rate of the OBS network by reducing the probability for contention to occur over the case when WDM is used in the optical layer (OBS/WDM) where there is an upper bound to the number of wavelengths available in a given spectral region. Next, we thoroughly study the performance of the proposed OBS/SAC-OCDMA system in both MAC and optical layers. In addition, we evaluate the effect of adding code converters in the resources of the core node on the overall performance of the system. Finally, throughout the performance evaluation of the proposed system, we target the optimum number of codes with which the system should be designed at different traffic conditions in order to achieve the minimum possible value for the overall burst error rate.

978-1-4244-4148-8/09/$25.00 ©2009
This full text paper was peer reviewed at the direction of IEEE Communications Society subject matter experts for publication in the IEEE "GLOBECOM" 2009 proceedings.

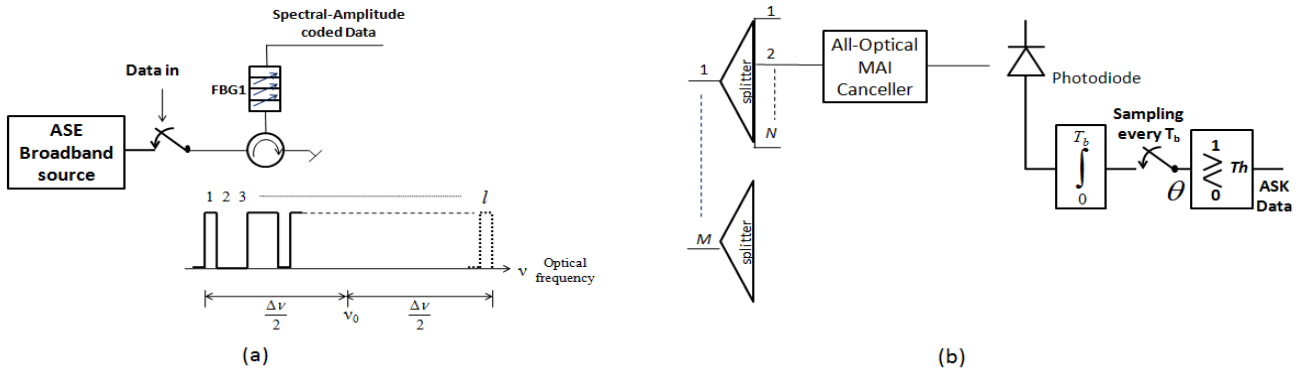

Fig.2. Architecture of an edge (ingress/egress) node in OBS/SAC-OCDMA system.

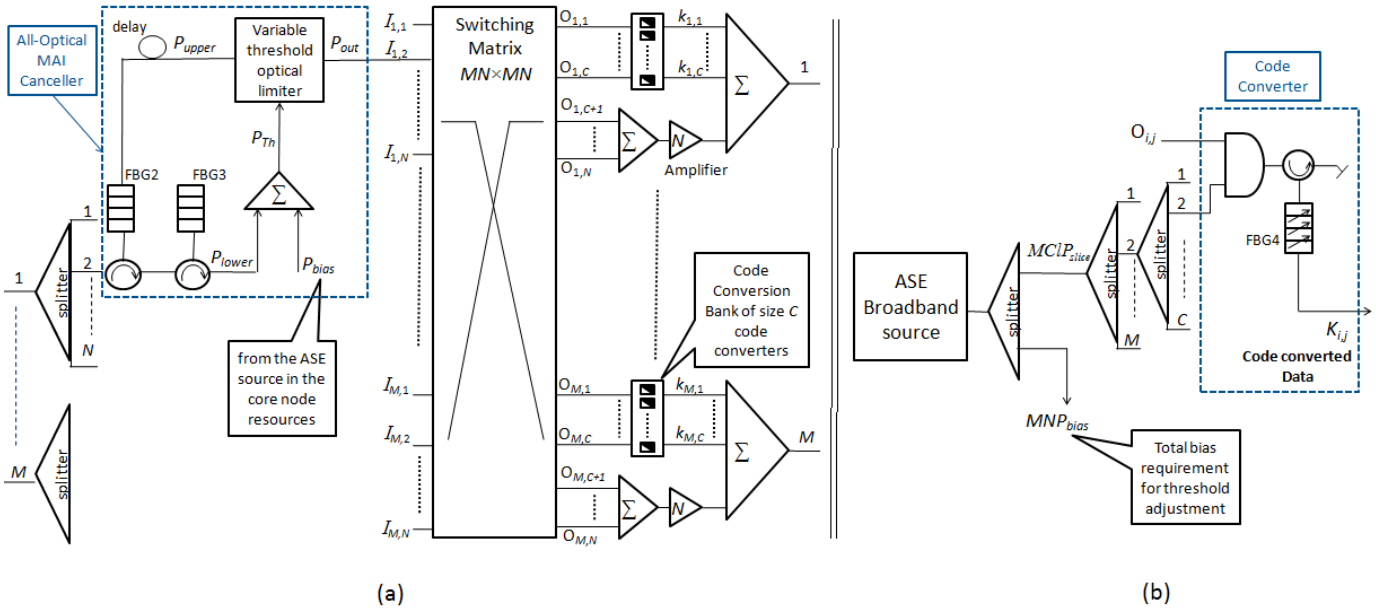

Fig.3. Architecture of a core node in OBS/SAC-OCDMA system.

The remainder of this paper is organized as follows. In Section II, we present a detailed description for our proposed system (OBS/SAC-OCDMA). Section III is devoted for the performance evaluation of the proposed system. In Section IV, numerical results for the derived performance measures are introduced. Finally, we give our conclusion in Section V.

II. System Description

A. Basics of OBS with SAC-OCDMA

In the OBS/WDM network, the CP contains two main fields of information; the wavelength on which the upcoming DB will arrive, and the destination to which this DB should be forwarded. These two fields of information are essential for the core node to bypass the DB to the destined output port.

However, in our proposed OBS/SAC-OCDMA system, we rely on multiplexing different DBs in the code domain rather than on the wavelength domain in the ordinary OBS/WDM system. Thus, the CP should contain information about the code used to mask the spectrum of the source during the transmission of its corresponding DB instead of the wavelength. Based on the code, and destination information in the CP, the core node will be capable of forwarding the DB to the proper output port in the so called code-based forwarding process which is explained in details later in this section.

B. Ingress node description:

In our newly proposed system, the ingress node has an additional mission rather than computing the offset time and assembling the packets into DBs; it should (through the burst scheduler in Fig. 1) assign a code to the DB before transmission and adjust the spectral encoder to mask the spectrum produced by the broadband amplified spontaneous emission (ASE) source with the assigned code. This broad bandwidth Δν is divided into l slices to be encoded according to the code assigned by the scheduler. We assume that the power distribution of the ASE source is flat over the spectrum which means that $P_{slice} = P_{ASE\_ingress}/l$, where $P_{ASE\_ingress}$ is the total power emitted from the ASE source placed at the ingress node and P_{slice} is the power of one spectral slice. The codes deployed in our system are generated from a Hadamard matrix of size $l \times l$. We denote by N the number of codes that are currently in use in the system which has a maximum value of $l - 1$ where all the rows of the Hadamard matrix are assigned to different DBs except the first row.

In Fig. 2a, a schematic diagram shows the spectral encoder at the ingress node where the DB is encoded with one of the N codes using the tunable chirped fiber Bragg grating (FBG1). In the encoding process of the DB, FBG1 is tuned to mask the spectrum produced by the ASE source with the assigned code.

978-1-4244-4148-8/09/$25.00 ©2009
This full text paper was peer reviewed at the direction of IEEE Communications Society subject matter experts for publication in the IEEE "GLOBECOM" 2009 proceedings.

This is done via passing certain slices in the spectrum according to the mark positions of the assigned code while reflecting the slices that correspond to the space positions in the code. The switch shown in Fig. 2a performs the On-Off Keying (OOK) of the input data by bypassing the spectrum of the ASE source to FBG1 when a data '1' is sent and prevents the spectrum from passing to FBG1 when a data '0' is sent. Thus, the encoder emits a signal power $lP_{slice}/2$ when a data '1' is sent while it produces no power when a data '0'is sent.

C. Core (intermediate) node description:

According to Fig.1, the core node operation lies in both the MAC and optical layers. Operation in the MAC layer involves CP processing and extracting the information required for bypassing the corresponding DB (code assigned, time of arrival, and destination). However, operation in the optical layer involves the reception and retransmission of the received spectrally encoded data, MAI cancelation process and power adjustment in order to perform the code-based forwarding process.

It is assumed that the core node has equal number of M input and output ports as shown in Fig. 3a. A splitter is placed at each input port to split the received signal over N paths. Each path contains an all-optical MAI canceller which aims to extract the desired DB, which has been assigned a specific code that is dedicated to this path, from its interferers. The all-optical MAI canceller comprises of two chirped FBGs (FBG2 and FBG3) where FBG2 is designed to pass the part of the spectrum that corresponds to the marked positions of the specific code and reflect the power on the space positions (the complement) of the DB's code, while FBG3 is designed to align the spectrum slices reflected from FBG2 in time. The delay in the upper branch is introduced to compensate the round-trip delay introduced by FBG2 and FBG3, hence realign the two spectra on the two branches in time.

The key idea of the reception of a spectrally encoded signal in an SAC-OCDMA system is to make the interferers cancel themselves, which is based on the fact that the Hadamard codes have the property that an interfering code overlaps with the desired code and its complement in exactly $l/4$ mark positions, where l is the code length. Applying this property, we can formulate the power levels in the upper and lower branches, shown in Fig.3a, P_{upper} and P_{lower} respectively as follows:

$$P_{upper} = \begin{cases} \frac{lP_{slice}}{4N}\left(N_{interf}+2\right) & '1'sent \\ \frac{lP_{slice}}{4N}N_{interf} & '0'sent \end{cases}$$

$$P_{lower} = \frac{lP_{slice}}{4N}N_{interf}$$

where N_{interf} denotes the number of interferers. By making use of that property, the MAI will be eliminated by subtracting the two signal powers on the two branches P_{upper} and P_{lower}. The key component in the all-optical MAI canceller is the variable threshold optical limiter whose functionality is equivalent to this subtraction process where it hard limits P_{upper} according to the variable threshold power P_{Th} which is controlled by P_{lower}. This implies that the optimum value of P_{Th} should be set at the middle of the range between P_{upper} and P_{lower}, i.e. $P_{Th} = \frac{lP_{slice}}{4N}\left(N_{interf}+1\right)$. Hence, an active power P_{bias} equal to $lP_{slice}/4N$ introduced by an ASE source placed at the core node shown in Fig. 3b is combined with P_{lower} to adjust its value to reach the optimum P_{Th}. Specifically, the required characteristics of the variable threshold optical limiter is given as follows:

$$P_{out} = \begin{cases} \frac{lP_{slice}}{2N} & P_{upper} > P_{Th} \\ 0 & P_{upper} < P_{Th} \end{cases} \quad (1)$$

In order to resolve the probable contention at each output port, we deploy a code conversion bank that comprises of c code converters, where $c < N$, ready to be shared by the DBs forwarded to this output port, i.e. a Share-Per-Line (SPL) strategy is adopted as shown in Fig. 3a. The operation of each code converter in the bank is separately illustrated in Fig. 3b where it acts as a spectral encoder that retransmits the data on the output line $O_{i,j}$ of the switching matrix, where $i \in \{1,2,\dots,M\}$ and $j \leq c$, by encoding the spectrum of the power fed by the ASE source through the AND gate [5] controlled by the data on the output line $O_{i,j}$ with a free code to which the original DB's code shall be converted. Finally, we should note that the power level at the output of the code converter equals $lP_{slice}/2$ given that the data on $O_{i,j}$ is '1' while no power is emitted if the data on $O_{i,j}$ is '0'.

In the above discussion, the number of code converters is limited to c, where $c < N$, which means that partial code conversion capability is employed. This is justified by two restrictions that sophisticate the implementation of large number of code converters in the bank. First, the power budget needed from the ASE source in the core node is proportional to c. Second, the cost of implementation of such an advanced technology of the tunable chirped FBGs also increases with increasing the value of c. Another issue regarding the partial code conversion is that the power level at each of the output lines of the code converters $K_{i,j}$ is different from that on the output lines of the switching matrix $O_{i,j}$ for $c < j \leq N$. Thus, an amplifier is introduced to the lines $O_{i,j}$, where $c < j \leq N$, that did not undergo the code conversion process in order to boost them to the power level at $K_{i,j}$. Finally, the total power requirement from the ASE source that should be placed at the core node equals $cMlP_{slice} + MNP_{bias}$.

D. Egress node description:

It is assumed that the egress node has M input ports; each port is introduced to a splitter which splits the input power to N paths, each of which is dedicated to a specific code reception. The cancellation of the MAI is performed optically through the proposed all-optical MAI canceller and the receiver makes the decision only in the electronic domain. After the MAI canceller, the output power that strikes the photodetector in the egress node is either lP_{slice} / $2N$ if a data '1' is sent or zero if a data '0' is sent. Finally, a decision can be made using the circuitry shown in Fig. 2b via comparing the sampled output from the integrate and dump circuit against a certain threshold value. After every bit in the DB is received, the DB is disassembled back to its original data packets, each of them can be directed to its own destination. However, the decision made in the electronic domain still might be erroneous due to the existence of the photodetector thermal, shot and dark current noises as will be handled later in the performance evaluation of the system.

978-1-4244-4148-8/09/$25.00 ©2009
This full text paper was peer reviewed at the direction of IEEE Communications Society subject matter experts for publication in the IEEE "GLOBECOM" 2009 proceedings.

III. PERFORMANCE EVALUATION OF THE OBS/SAC-OCDMA SYSTEM

As shown in Fig.1, operation of the OBS/SAC-OCDMA system involves both MAC and optical layers. Hence, for a DB to be correctly received, success should be achieved by the DB while transmission in the optical layer provided that its corresponding CP has already succeeded in the MAC layer.

A. Performance of the OBS/SAC-OCDMA system in the MAC layer

As mentioned earlier, for a DB to be received in success at its egress node, its corresponding CP should successfully reserve resources at all core nodes lying on its route extending from the ingress node to the egress node. To evaluate the performance of the OBS/SAC-OCDMA system in the MAC layer, we study the performance of a single core node in the CP path by calculating the *per-node burst loss probability* $P_{Node\text{-}Loss}$ from which we calculate the *MAC burst loss probability* $P_{MAC\text{-}Loss}$ which measures the overall performance of all nodes lying between ingress and egress nodes.

A.1) Model assumptions

We perform a Markovian analysis to characterize the performance of a single core node. This analysis is carried out under the following assumptions:

- We assume that the destination for an incoming burst to the core node is uniformly distributed among all available output ports $(1:M)$. Thus, it is sufficient to model the behavior of a single output port.
- A core node is assumed to have the following resources:
  i. A single wavelength around which the ASE broadband source emits its light, which is the center frequency (v_0) of the coded spectrum as shown in Fig. 2a.
  ii. No fiber delay lines for contention resolution.
  iii. A number of N codes that can be used to serve the incoming burst arrivals.
  iv. A code converter bank at every output port, each of which comprises of c code converters shared between DBs forwarded to this port, where $c \in \{1,2,\dots,N\}$, i.e. a Share-Per-Line (SPL) strategy is adopted. Each code converter can convert an arriving DB on a given code to any other free code. We define the code conversion capability as $\gamma \stackrel{\text{def}}{=} \frac{c}{N}$ in order to discriminate between three different cases. The two limiting cases when $\gamma = 0$ and $\gamma = 1$ represent the cases of no and full code conversion respectively, whereas, if $0 < \gamma < 1$, the node has partial code conversion capability.
- Incoming DBs are assumed to arrive at the node according to a Poisson process with a mean arrival rate λ bursts/seconds. In addition, we assume the code on which an incoming DB arrives is uniformly distributed over $(1:N)$. Moreover, the service time of an incoming burst is assumed to have an exponential distribution with mean $1/\mu$ seconds which is the average duration of DB.

A.2) Model Equations for the limiting cases: no and full code conversion capability ($\gamma = 0$ & $\gamma = 1$)

For the case of full code conversion ($\gamma = 1$), each output port can be safely modeled as an M/M/N/N loss system with N servers modeling the N available number of codes. We can obtain the *per-node burst loss probability* $P_{Node\text{-}Loss}$, which is defined as the probability that a CP fails to reserve appropriate resources for its corresponding DB at a core node that lies on the path between the ingress and egress nodes, from the well known Erlang-B formula as follows:

$$P_{Node-Loss} = \frac{\rho^N / N!}{\sum_{i=0}^{N} \rho^i / i!} \quad (2)$$

where the offered load on all the available codes is:

$$\rho \stackrel{\text{def}}{=} \lambda/\mu$$

For the case of absence of code conversion ($\gamma = 0$), each output port can be reasonably modeled as N independent single server M/M/1/1 loss systems each with an offered load $\lambda/N\mu$. Hence, $P_{Node\text{-}Loss}$ can also be calculated via the Erlang-B formula as follows:

$$P_{Node-Loss} = \frac{\rho/N}{1 + \rho/N} \quad (3)$$

A.3) Model Equations for the partial code conversion capability ($0 \le \gamma \le 1$)

We are going to evaluate $P_{Node\text{-}Loss}$ in case of partial code conversion ($0 < \gamma < 1$) via a Markovian analysis carried out for a certain output port similar to that used in [6]. Let $i(t)$ and $j(t)$ denote the number of codes and the number of code converters inside the output port's converter bank that are in use at time t, respectively. The process $X(t) = \{(i(t), j(t)) : t \ge 0\}$ is a two dimensional continuous time Markov process (CTMC) on the state space $S = \{(i,j) : 0 \le i \le N, 0 \le j \le min(i,c)\}$. Now, let us assume that the process *X(t)* is currently at state (i,j) at time t, and knowing that DB arrivals occur with an average rate λ burst/seconds, one of three possible scenarios may take place if a DB arrives:

i. The code on which the DB arrives is currently free on the output port which is an event with a probability $(N-i)/N$ and the DB will be successfully served and the process will jump to state $(i+1, j)$ with a transition rate $\lambda\,(N-i)/N$.
ii. The DB's code is currently in use by another transmission on the desired output with a probability i/N, which will lead to one of two possibilities:
   - If $j = c$, the DB will be dropped because all code converters in the converter bank are busy which results in no state change.
   - If $j < c$, the DB will be successfully served by randomly assigning it to one of the free codes and converting it via one of the free code converters which leads to a state transition to state $(i+1, j+1)$ with a rate $\lambda \cdot i/N \cdot \left(1 - \lfloor j/c \rfloor\right)$.

Conversely, if the process *X(t)* is currently at state (i,j) at time t, given that DB departures occur with a rate $i\mu$ burst/seconds, one of two possible scenarios may arise if a DB departs the node:

i. The departing DB was using a code converter which is an event with a probability j/i, which leads to a transition to state $(i-1, j-1)$ with a rate $i\mu \cdot j/i$.

978-1-4244-4148-8/09/$25.00 ©2009
This full text paper was peer reviewed at the direction of IEEE Communications Society subject matter experts for publication in the IEEE "GLOBECOM" 2009 proceedings.

ii. The departing DB was not using a code converter with a probability $(i-j)/i$ leading to a transition to state $(i-1, j)$ with a rate $i\mu\,(i-j)/i$.

Next, we calculate the generator matrix Q that gives all possible transition rates for this CTMC in a similar approach to that proposed in [6] based on state decomposition into levels and generating Q by dividing it into sub-blocks representing transitions from a level to either the higher neighboring, lower neighboring or same level. Then, the steady-state probabilities of this CTMC $\pi_{i,j}$ can be found by solving the following system of equations:

$$\bar{\pi}Q = 0 \;\;,\;\; \bar{\pi}e = 1$$

where $\bar{\pi} = [\pi_{0,0},\, \pi_{1,0},\, \pi_{1,1},\, \pi_{2,0}, \cdots,\, \pi_{N,c}]$ and e is a column vector of ones of size $\left(N - {}^{c}/_{2} + 1\right)(c+1)$.

Then, the *per-node burst loss probability* $P_{Node-Loss}$ is obtained from the steady state probabilities as follows:

$$P_{Node-Loss} = \sum_{i=0}^{c} \pi_{N,i} + \sum_{j=c}^{N-1} \frac{j}{N} \pi_{j,c} \qquad (4)$$

Next, we assume the overall network traffic is uniformly distributed across the entire network, hence the offered load ρ and the *per-node burst loss probability* $P_{Node-Loss}$ can be safely assumed the same for all nodes. Consequently, one can obtain the *MAC burst loss probability* $P_{MAC\text{-}Loss}$, which is the probability that a CP fails in the reservation process at any of the nodes existing in its corresponding DB path, as follows:

$$P_{MAC-Loss} = 1 - (1 - P_{Node-Loss})^{H} \qquad (5)$$

where H is the maximum possible number of core nodes that a path can contain which is the worst case representing the longest possible path that can be established in the network, that results in the highest possible $P_{MAC\text{-}Loss}$. In equation (5), $P_{Node\text{-}Loss}$ is either given by equation (2) in case of presence of full code conversion, equation (3) in case of absence of code conversion or equation (4) in case of partial code conversion.

B. Performance of the OBS/SAC-OCDMA system in the optical layer

The performance in the optical layer depends mainly on the decision error that might originate from the receiver thermal, shot and dark current noises while photodetecting each bit in the desired DB.

The approach adopted to evaluate the performance of the OBS/SAC-OCDMA system in the optical layer is based on the assumption that success in the reception of a DB is contingent on the success in receiving all its contained bits. Hence, we evaluate the bit error rate, denoted BER_{PHY}, which is defined as the error rate encountered in the decision while receiving each bit. In order to calculate BER_{PHY}, we should obtain the probability distribution function $P_{\theta}(\theta)$ of the decision variable θ shown in Fig. 2b, which is the accumulated charge after the integrator in Coulombs. After that, one can easily write:

$$BER_{PHY} = \frac{1}{2}P_{e/1} + \frac{1}{2}P_{e/0}$$

which can be written as follows:

$$BER_{PHY} = \frac{1}{2}\int_{-\infty}^{Th} P_{\theta/1}(\theta)d\theta + \frac{1}{2}\int_{Th}^{\infty} P_{\theta/0}(\theta)d\theta \qquad (6)$$

where Th is the decision threshold.

The following are the list of variables with their definitions which are going to be used in the next part of the analysis:

T_b: Bit duration in seconds.
R_b: Bit rate.
η: Quantum Efficiency of the photodetectors.
i_d: Photodetector dark current.
h: Plank's constant.
v_0: Operating frequency.
e_0: Electron charge.
L_{burst}: Average burst length in bits.
$P_{ASE\_ingress}$: Emitted power from ASE source at the ingress node which also equals lP_{slice}.

We also assume a thermal noise with intensity N_0 (W/Hz), hence the variance of the output thermal noise of an integrator with integration duration of T_b seconds will be $\sigma^2 = N_0T_b/2$. Moreover, we denote by λ_d the dark current photoelectron rate of the photodetector. Therefore, the mean photoelectron count over a period of T_b seconds due to dark current will be λ_dT_b. We also denote by λ_s the photoelectron rate due to incident signal photons. Therefore, the mean signal photoelectron count over a period of T_b seconds will be λ_sT_b.

Based on the previous assumptions, one can easily write:

$$P_{\theta/b}(\theta) = \sum_{n=0}^{\infty} P(n/b)\frac{e^{\frac{-(\theta-ne_0)^2}{2\sigma^2}}}{\sqrt{2\pi\sigma^2}} \qquad (7)$$

and $$P(n/b) = Pos(n, b\lambda_sT_b + \lambda_dT_b)$$

where b is the transmitted bit, $\lambda_s = \frac{\eta P_{ASE\_ingress}}{2hv_0N}$, $\lambda_d = \frac{i_d}{e_0}$ and $Pos(n, X)$ denotes Poisson distribution with a mean X.

Here, we should note that while calculating λ_s, we divide by 2, which is justified by the fact that only half of the spectrum is transmitted given '1' sent while the other half is masked. Another issue while calculating λ_s is dividing by N in order to consider the effect of the splitting performed at the front end of the egress node. On the other hand, other splitting operations performed at the front end of each core node in the path have no effect on the received signal power because the signal is effectively regenerated at each core node.

Next, we calculate BER_{PHY} by substituting from (7) into (6) and performing the integration, we get:

$$BER_{PHY} = \frac{1}{2}\sum_{n=0}^{\infty}\left(\frac{{G_1}^n}{n!}e^{-G_1} \times \frac{1}{2}erfc\left(\frac{e_0n - Th}{\sqrt{2}\sigma}\right)\right) + \frac{1}{2}\sum_{n=0}^{\infty}\left(\frac{{G_0}^n}{n!}e^{-G_0} \times \frac{1}{2}erfc\left(\frac{Th - e_0n}{\sqrt{2}\sigma}\right)\right) \qquad (8)$$

where $G_b = b\lambda_sT_b + \lambda_dT_b$

Finally, we calculate the *burst error rate*, denoted $BurstER_{PHY}$, which is defined as the error rate encountered while receiving DBs due to single bit errors, from BER_{PHY} by averaging over all possible values of the burst duration as follows:

$$BurstER_{PHY} = \int_0^{\infty}[1 - (1 - BER_{PHY})^{R_bt}] \times \mu e^{-\mu t}\,dt = 1 - \frac{1}{1 - L_{burst}ln(1 - BER_{PHY})} \qquad (9)$$

978-1-4244-4148-8/09/$25.00 ©2009
This full text paper was peer reviewed at the direction of IEEE Communications Society subject matter experts for publication in the IEEE "GLOBECOM" 2009 proceedings.

C. Overall performance of the OBS/SAC-OCDMA system in both layers

In this part, we study the overall performance of the proposed OBS/SAC-OCDMA system in both MAC and optical layers. This is based on the fact that the success of a DB mandates the success of the DB in the optical layer given that its CP has succeeded in the MAC layer. After the calculation of the *MAC burst loss probability* $P_{MAC\text{-}Loss}$ from equation (5) and the *burst error rate* $BurstER_{PHY}$ from equation (9), one can get the *overall burst error rate* $BurstER_{overall}$ from the following equation:

$$BurstER_{overall} = 1 - (1 - P_{MAC-Loss})(1 - BurstER_{PHY}) \quad (10)$$

IV. RESULTS

By employing the results obtained in equations (3) and (4), a comparison between the newly proposed OBS/SAC-OCDMA system and the ordinary OBS/WDM system in terms of the MAC *per-node burst loss probability* $P_{Node\text{-}Loss}$ can be held at different number of code and wavelength converters employed respectively. Furthermore, in order to make the comparison somewhat fair, we assume a spectral band $\Delta\nu$ equivalent to a 20 nm linewidth to be utilized for operation in both systems. For the OBS/WDM system, the number of channels within the 20 nm band of operation is assumed to be 25 by applying the fact that the typical channel bandwidth in DWDM is 0.8 nm (ITU standard). Conversely, the number of spectral slices within the 20 nm band of operation for the OBS/SAC-OCDMA system is assumed 64 as in [7] as it depends on the technology of fabrication of the chirped FBGs in the spectral encoder. Finally, we assume an average burst length L_{burst} of 10 Mbits.

Based on the previous assumptions, $P_{Node\text{-}Loss}$ is plotted in Fig. 5 versus ρ in order to compare between the two systems at different number of code and wavelength converters. Results reveal that employing SAC-OCDMA in the optical layer has a significant advantage over the ordinary WDM in terms of lower $P_{Node\text{-}Loss}$ for all traffic conditions. Moreover, we observe that the difference between the two systems is much more evident in the case of presence of code conversion. This is due to the better utilization of the extra number of servers in the OBS/SAC-OCDMA system by employing converters noting that code conversion imposes less complex implementation requirements when compared to wavelength conversion.

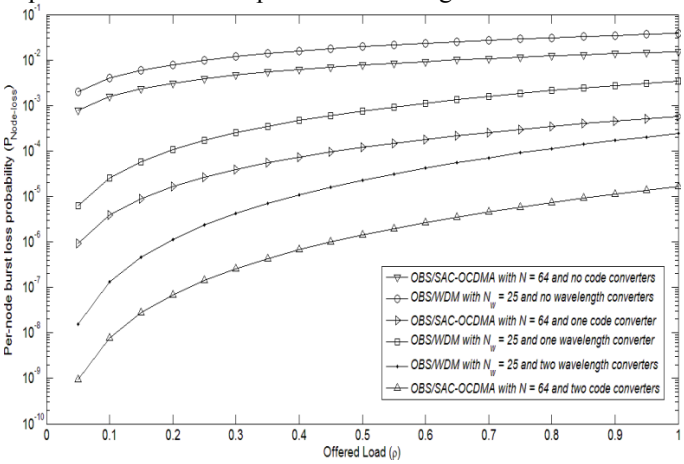

Fig. 5. Semi-log plot for MAC layer *per-node burst loss probability* versus the Offered Load for OBS/SAC-OCDMA and OBS/WDM systems at different number of code and wavelength converters.

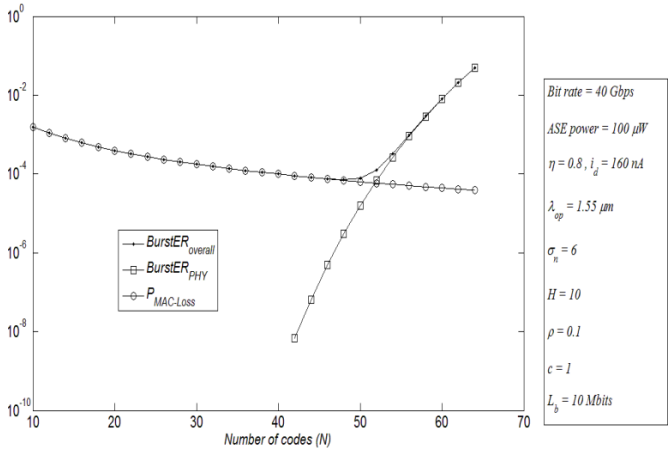

Fig. 6. Semi-log plot of *MAC burst loss probability*, optical layer *burst error rate* and *overall burst error rate* versus the available number of codes for OBS/SAC-OCDMA system with one code converter.

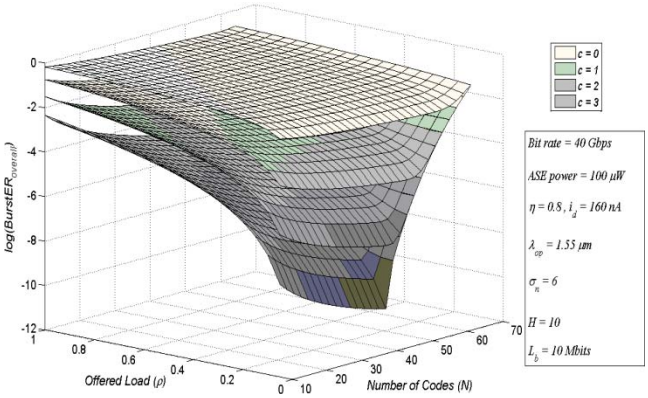

Fig. 7. Log *overall burst error rate* versus both the available number of codes and the offered load for OBS/SAC-OCDMA system at different number of code converters.

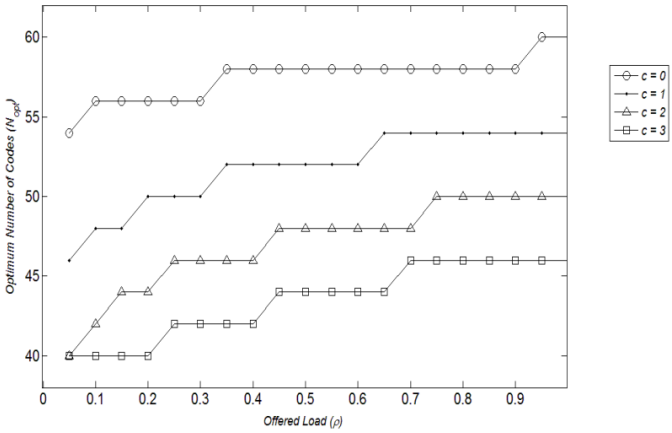

Fig. 8. Optimum number of codes versus the offered load at different number of code converters employed.

Another observation can be made from Fig. 5 is that code conversion effectiveness for low traffic values is superior when comparing it with the case of high traffic values. This is because when the traffic arrival rate is low; there will be more free codes to which the contending bursts can be converted.

Utilizing the results obtained in equations (5), (9) and (10), Fig. 6 shows $P_{MAC\text{-}Loss}$, $BurstER_{PHY}$ and $BurstER_{overall}$ versus the number of codes N deployed in an OBS/SAC-OCDMA system having one code converter. Furthermore, values of $BurstER_{PHY}$ are calculated when the threshold value Th is set to its optimum value which is found via a genetic algorithm based optimization. In Fig. 6, it is apparent that $P_{MAC\text{-}Loss}$

978-1-4244-4148-8/09/$25.00 ©2009
This full text paper was peer reviewed at the direction of IEEE Communications Society subject matter experts for publication in the IEEE "GLOBECOM" 2009 proceedings.

decreases when using larger number of codes because it is more probable for a CP to succeed in the reservation process when the available number of codes increases. Conversely, $BurstER_{PHY}$ increases with the increase of the number of codes N which is justified by the presence of the 1: N splitter at the front end of the egress node; hence, using more codes enlarges the splitting ratio leading to a lower received power level incident on the photodetectors which raises the probability for decision errors. Combining both $P_{MAC\text{-}Loss}$ and $BurstER_{PHY}$, we find that $BurstER_{overall}$ has an exciting relation with the number of codes N. For small values of N, $P_{MAC\text{-}Loss}$ dominates the overall error performance as compared to $BurstER_{PHY}$; hence, $BurstER_{overall}$ decreases with increasing N just like the behavior of $P_{MAC\text{-}Loss}$. On the other hand, for large values of N, $BurstER_{PHY}$ dictates the overall error performance forcing $BurstER_{overall}$ to increase with the increasing value of N. Intuitively, there is a minimum value for $BurstER_{overall}$ which is clearly the optimum design point, i.e. one should set the number of codes used in the system to the proper value that results in the least achievable $BurstER_{overall}$.

Next, Fig. 7 is a surface representing $BurstER_{overall}$ as a function of both the number of codes N and the offered load ρ for the OBS/SAC-OCDMA system at different number of code converters. For each value of c, it is obvious that there always exists an optimum value for N at each ρ leading to the minimum possible $BurstER_{overall}$ at this specific traffic condition when c code converters are used. Moreover, the efficacy of code conversion is quite evident from this figure as it is clear that introducing one more code converter enhances the overall performance of the system by decreasing $BurstER_{overall}$ significantly. In addition, we observe that this reduction in $BurstER_{overall}$ is much greater for lower traffic values. For example, at $N = 10$ and $\rho = 0.1$, $BurstER_{overall} = 10^{-1.024}$ for $c = 0$ and $BurstER_{overall} = 10^{-2.807}$ for $c = 1$. On the other hand, at $N = 10$ and $\rho = 1$, $BurstER_{overall} = 10^{-0.2115}$ for $c = 0$ and $BurstER_{overall} = 10^{-0.775}$ for $c = 1$. Another issue concerning Fig. 7 is that the optimum number of codes N_{opt} decreases clearly when more code converters are employed. For example, at $\rho = 0.05$, $N_{opt} = 46$, 42 and 40 for $c = 1$, 2 and 3 respectively. This observation is justified by the fact that adding more code converters decreases $P_{MAC\text{-}Loss}$ which shortens the range of dominance of $P_{MAC\text{-}Loss}$ over $BurstER_{PHY}$ leading to a smaller value of N_{opt}.

At last, Fig. 8 shows N_{opt} targeted for system design against the offered load ρ for different values of code converters c. It is clear that N_{opt} is larger for heavier traffic conditions. This is due to the dominance of the $P_{MAC\text{-}Loss}$ over $BurstER_{PHY}$ for heavier traffic values which corroborates the effectiveness of adding more codes in order to reduce $P_{MAC\text{-}Loss}$ (the dominant error component). Another interesting observation from Fig. 8, given a certain number of code converters used, the value of N_{opt} remains constant for a certain range of ρ, which is very promising because the value of N_{opt} at which the system should be operated at a certain traffic condition remains also optimum when the traffic conditions change slightly, i.e. achieving a robust design for our system in terms of N_{opt} is feasible.

V. CONCLUSION

We propose a new contention resolution technique for OBS networks by employing SAC-OCDMA instead of WDM in the optical layer underneath OBS in the MAC layer. Results show that the newly proposed OBS/SAC-OCDMA system outperforms the previous OBS/WDM system in terms of *per-node burst loss probability*. In addition, employing code converters enhances the proposed system performance noticeably especially for low traffic scenarios. Furthermore, an all-optical MAI cancellation is proposed. Finally, we observe that the *overall burst error rate* of the system is minimum at certain values for the employed number of codes which are the optimum points at which the system should be operated.

Considering the complexity of the proposed system, employing code converters is contingent on the availability of tunable chirped FBGs which are practically available as reported in [8]. Another issue related to system complexity is the practical limitation imposed by the variable threshold optical limiters on our proposed system; however, researchers in [9] reported the availability of such devices. More efforts are expected to realize practical variable threshold limiters in the near future. Finally, our proposed system is also disadvantageous somehow in that it requires an ASE broadband source at each node. Such active elements required increase the overall power requirement in the network; however, ASE broadband sources with large output power levels are practically available. Furthermore, the power required from each ASE source in the core node increases linearly with the deployed number of converters in the node, which is the price paid for the tremendous improvement achieved in the overall system performance by adding code converters. Despite the proportionality between the total power requirement and the number of code converters, we should note that a tiny number of code converters can achieve a huge improvement in the performance as the numerical results suggested, while at the same time having a small impact on the overall power requirement in the network.

REFRENCES

[1] C. Qiao and M. Yoo, “Optical burst switching (OBS)—A new paradigm for an optical internet,” *J. High SpeedNetw.*, vol. 8, no. 1, pp. 69–84, Jan. 1999.

[2] T. Battestilli and H.Perros, “An Introduction to Optical Burst Switching,” *IEEE Commun. Mag.*, vol.41, pp. S10- S15 2003.

[3] K. Kamakura, O. Kabranov, D. Makrakis and I. Sasase, “OBS Networks Using Optical Code Division Multiple Access Techniques”, *ICC'04*, pp.1725-1729, Paris, France, June 2004.

[4] M. Kavehard and D. Zaccarin, "Optical Code-Division-Multiplexed Systems Based on Spectral Encoding of Noncoherent Sources", *JLT*, vol. 13, no. 3, pp. 534-545, 1995.

[5] X.Zhang et al., “All-optical AND gate at 10 Gbit/s based on cascaded single-port-couple SOAs”, *Optics Express*, 2004.

[6] N. Akar, E. Karasan and K. Dogan, “Wavelength converter sharing in asynchronous optical packet/burst switching: an exact blocking analysis for Markovian arrivals,” *J-SAC,* vol.24, no. 12, pp. 69-80, Dec. 2006.

[7] E. Smith, R. Blaikie and D. Taylor, "Performance Enhancement of Spectral-Amplitude-Coding Optical CDMA Using Pulse-Position Modulation", *IEEE Trans. on Communications*, vol. 46, no. 9, pp. 1176-1185, 1998.

[8] S.Y. Set, B. Dabarsyah, C.S. Goh, K. Katoh, Y. Takushima and K. Kikuchi, “A widely tunable fiber Bragg grating with a wavelength over 40 nm,” *OFC 2001*.

[9] H. Goto, *et al.*, "Unitary Variable Threshold Optical Limiter without Bulky Optical Systems", *IEEE CLEO* 2007.

978-1-4244-4148-8/09/$25.00 ©2009

This full text paper was peer reviewed at the direction of IEEE Communications Society subject matter experts for publication in the IEEE "GLOBECOM" 2009 proceedings.